J. Am. Chem. Soc. **1982**, *104*, 7436–7441

Collision-Induced Dissociation of Proton-Bound Alcohol Dimers by Fourier-Transform Mass Spectrometry

R. C. Burnier, R. B. Cody, and B. S. Freiser*

Contribution from the Department of Chemistry, Purdue University, West Lafayette, Indiana 47907. *Received December 21, 1981*

Abstract: Fourier-transform mass spectrometry is used to obtain quasi-breakdown curves for the low-energy collisional activation of mass-selected proton-bound dimers of a few simple aliphatic alcohols, viz., *n*-C_3H_7OH, *i*-C_3H_7OH, *n*-C_4H_9OH, *sec*-C_4H_9OH, *t*-C_4H_9OH, *t*-$C_5H_{11}OH$, and *neo*-$C_5H_{11}OH$. These breakdown curves facilitate the examination of gas-phase ions in terms of their structure and energetics. The unimolecular fragmentation behavior of ions undergoing collisional activation, the bimolecular reaction at thermal energies, and the multiphoton activation in the infrared are compared. Decomposition pathways having high energies of activation that are observed by ion–molecule reactions and multiphoton dissociation are sometimes not observed by low-energy collisional activation. In spite of this limitation, low-energy CID is found to be a powerful method for delineating isomeric structures. The ease of dehydration of proton-bound dimers of alcohols in the gas phase by collisional activation is found to follow the same order for their acid-catalyzed dehydration in solution: tertiary > secondary > primary. A brief discussion of multicollisional effects is also presented.

For several years the investigations of high-energy collisions of ions with neutral particles have proved invaluable in providing the mass spectroscopist with information regarding ion identification and structure. Moreover, these ion–molecule reactions provide insight into the nature of excitation and decomposition along the reaction coordinate. Many such collision-induced dissociation (CID) processes are characterized by ions possessing internal energy sufficient to make accessible several competitive reaction channels.

Recently it has been shown that variations in product ion branching ratios with translational energy of the colliding ion are smaller in the high-energy collision manifold (1–10 keV) than in the low-energy (1–100 eV) regime.[1] High-energy CID processes are thought to occur via electronic excitation with a minimal transfer of momentum to the target. Low-energy CID processes involve complex formation with the target and result in appreciable momentum transfer. The amount of internal energy deposited in the ion, however, is comparable in both cases. Of significance is the good correspondence between the collision energy for both processes and ion internal energy. Plots of ion abundance vs. internal energy compare reasonably well with branching ratios for competitive CID reactions plotted as a function of kinetic energy. Therefore, a careful control of kinetic (collision) energy yields a similar control of ion internal energy and a means for probing unimolecular kinetics.

The analyses of these reactions by tandem instruments such as the triple quadrupole (QQQ),[2] magnetic sector quadrupole (BQ), QQ, and BQQ[1] mass spectrometers are a relatively new development. More recently, our laboratory has utilized the technique of Fourier-transform mass spectrometry (FT/MS) to investigate low-energy CID reactions.[3] In an effort to gain a better understanding of the fundamental nature and applications of the technique, we chose to study the unimolecular decompositions of a few proton-bound dimers of aliphatic alcohols. This study parallels that of Beauchamp et al.,[4] who demonstrated the ability to probe potential energy surfaces and ion structures by employing a low-power continuous-wave infrared laser to irradiate gas-phase ions in an ion cyclotron resonance (ICR) spectrometer. It was shown that proton-bound alcohol dimers undergo a slow sequential multiphoton absorption and decompose primarily by the lowest-energy pathway. In the present study, complementary information is provided by varying the internal energy over a wider range. The ability to vary translational energy provides a method to distinguish isomers, especially when they yield similar CID products, and to examine potential surfaces of bimolecular reactions in a fashion similar to the multiphoton approach, but lacking the constraint of requiring absorption. Differences between multiphoton decompositions (MPD) and CID at low-energy thresholds are observed and may be attributed to the nature and amount of energy deposition and the resulting fragmentation efficiency for each process.

Experimental Section

The theory, instrumentation, and methodology of FT/MS and conventional ICR spectroscopy[5,6] have been discussed at length elsewhere. Measurements were made on a prototype of the Nicolet FT/MS-1000 with a 1-in. cubic cell similar to that previously described by Comisarow.[5] The spectrometer utilizes a 15-in. electromagnet maintained at a fixed, nominal magnetic field of 0.9 T. Sample and target gases were introduced via a triple inlet system, and pressure was measured by a Varian Bayard-Alpert type ionization gauge. Sample pressures ranged from 1×10^{-7} to 1×10^{-6} torr; target gas pressures ranged between 2×10^{-6} and 1×10^{-5} torr. Only high-purity, degassed, commercial reagents were used.

The present experiments are controlled by a Nicolet 1180E computer with 128K of memory and two disk drives. The maximum digitization rate is 5.0 MHz with 12-bit resolution. A Nicolet programmable frequency synthesizer generates all of the radio frequency (RF) pulses.

The timing sequence used in the present experiments is generalized in Figure 1. The experiment begins with a quench pulse that purges the cell of any ions. This is accomplished by biasing the left and right trapping plates at +15 and −15 V, respectively. Next, an ion-formation pulse occurs. This typically consists of a 20-ms, 13-eV, electron-beam pulse. Two separate double-resonance pulses, DR_1 and DR_2, may then be applied to eject either one ion or several ions, depending on whether the pulses are set at a discrete frequency or swept over a range of frequencies. A third double-resonance pulse performs the task of accelerating the ion of interest to a particular kinetic energy. The total acceleration time is either 100 or 500 μs. Immediately following DR_3 there is a delay (hereafter called the CID interaction time) of anywhere between 10 and 100 ms during which time collision-induced dissociation

(1) McLuckey, S. A.; Glish, G. L.; Cooks, R. G. *Int. J. Mass Spectrom. Ion Phys.* **1981**, *39*, 219.

(2) (a) Yost, R. A.; Enke, C. G. *J. Am. Chem. Soc.* **1978**, *100*, 2274. (b) Yost, R. A.; Enke, C. G., *Anal. Chem.* **1979**, *51*, 1251A. (c) Yost, R. A.; Enke, C. G.; McGilvery, D. C.; Smith, D.; Morrison, J. D., *Int. J. Mass Spectrom. Ion Phys.* **1979**, *30*, 127.

(3) (a) Cody, R. B.; Freiser, B. S. *Int. J. Mass Spectrom. Ion Phys.* **1982**, *41*, 199. (b) Cody, R. B.; Burnier, R. C.; Freiser, B. S. *Anal. Chem.* **1982**, *54*, 96.

(4) Bomse, D. S.; Beauchamp, J. L. *J. Am. Chem. Soc.* **1981**, *103*, 3292.

(5) (a) Comisarow, M. B.; Marshall, A. G. *J. Chem. Phys.* **1976**, *64*, 110. (b) Comisarow, M. B. *Int. J. Mass Spectrom. Ion Phys.* **1981**, *37*, 251. (c) Comisarow, M. B. *Adv. Mass Spectrom.* **1980**, *8*, 1698. (d) Ghaderi, S.; Kulkarni, P. S.; Ledford, E. B.; Wilkins, C. L.; Gross, M. L. *Anal. Chem.* **1981**, *53*, 428.

(6) (a) Lehman, T. A.; Bursey, M. M. "Ion Cyclotron Resonance Spectrometry"; Wiley-Interscience: New York, 1976. (b) Beauchamp, J. L. *Annu. Rev. Phys. Chem.* **1971**, *22*, 527.

0002-7863/82/1504-7436$01.25/0

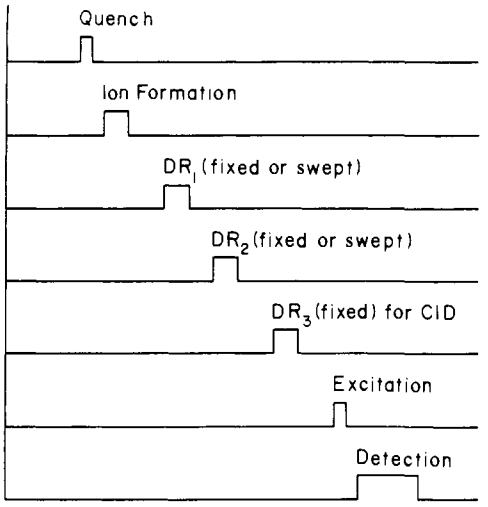

Figure 1. Typical sequence of events for the FT/MS CID experiment.

can occur. This interaction time is adjusted to maximize the signal due to CID while ensuring that none of the daughter ions have reacted. The time delay between the ion formation pulse and DR_1 serves as the "trapping time" during which these reactions can take place. During the excite pulse, an RF "chirp" (typically 0–1 MHz in 1 ms) is used to accelerate all of the ions coherently. A real-time signal is generated during the subsequent detect pulse which is amplified and digitized. The sequence is then repeated. The time-averaged signal is Fourier transformed, yielding a mass spectrum that can be stored on a disk and later reloaded into the memory with all of the original parameters retained.

The RF amplitude, the delay times between pulses, and the duration of the pulses are independent and computer selected. Variation of the translational energy of ions undergoing CID is accomplished by varying either the RF amplitude or duration. The former method was employed here except for the data obtained in Figure 7. The CID efficiency is less than 100%, and typically, a maximum of 50% conversion of dimer ions to decomposition products is obtained. The maximum amount of kinetic energy imparted to an ion in FT/MS is given by eq 1

$$E_{tr} = E_{RF}^2 e^2 t^2 / 8m \qquad (1)$$

and is limited to being less than that required to totally eject the ion from the cell.[3b,6a] Here E_{RF} is the electric field in volts per meter, e is the electronic charge in coulombs, t is the duration in seconds over which the ion is irradiated by the RF pulse, and m is the mass of the ion in kilograms. Since the maximum attainable translational energy is inversely proportional to the ionic mass, the energy range over which high mass ions can be accelerated is reduced with respect to those of lower mass. Fortunately, proton-bound alcohol dimers dissociate readily at energies below the upper limit at which ion ejection occurs.

The results for a typical CID experiment are illustrated in Figure 2. Shown in the figure is the spectrum that arises following 13-eV electron-impact ionization on a mixture of *sec*-butyl alcohol at 2×10^{-7} torr and N_2 at 6×10^{-6} torr with a 1-s trapping time. Besides the proton-bound alcohol dimer at M/z 149, a number of other ions are observed as expected from earlier reported studies.[7-10] Figure 2b shows the spectrum obtained under the same conditions as in Figure 2a except that a double-resonance pulse, swept at 40 Hz/μs, is applied over a frequency range that corresponds to a mass range between 40 and 133 amu. With a suitable RF amplitude (3.8 V), removal of all ions except M/z 149 is accomplished. Application of a second double-resonance pulse for 100 μs and at an RF level of 2.1 V, 40 ms prior to the RF chirp, accelerates the proton-bound dimer to a translational energy of 5.53 eV. Within the 40 ms, the CID event can take place yielding, in this case, decomposition products at M/z 131, 93, 75, and 57 as shown in Figure 2c. The amplitude and duration of the RF pulse greatly affects the ratio of these products. The dependence on RF level (kinetic energy) for the proton-bound dimer of *sec*-butyl alcohol is shown in Figure 3 and indicates that

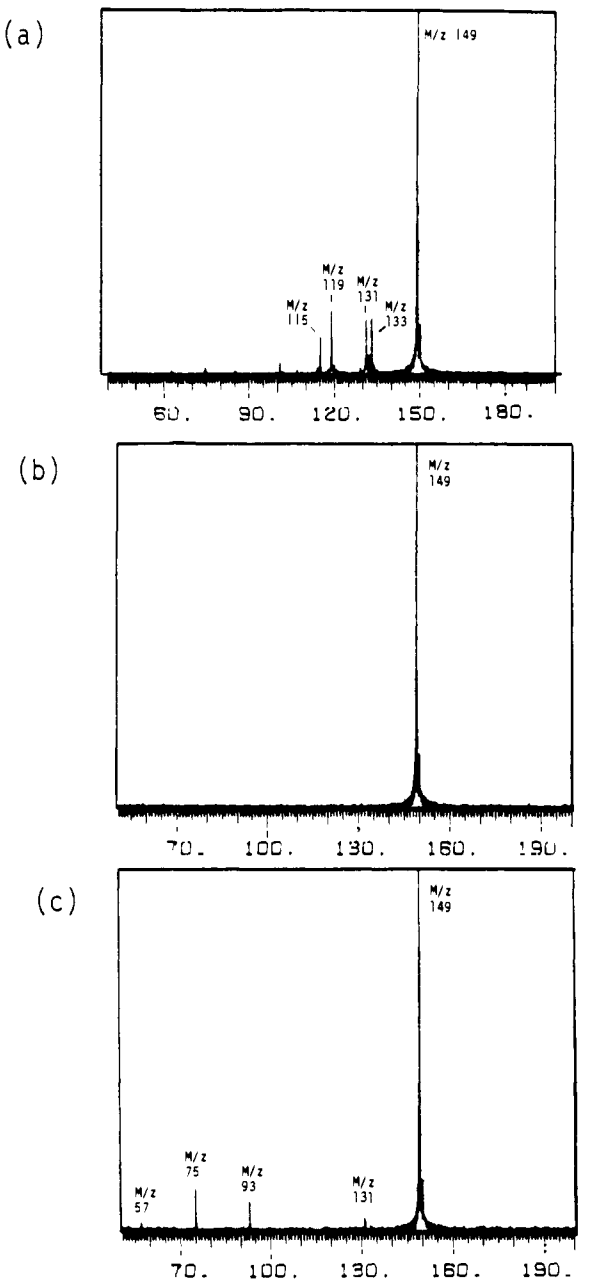

Figure 2. (a) Mass spectrum obtained from a mixture of *sec*-butyl alcohol at 2×10^{-7} torr and N_2 at 6×10^{-6} torr with a nominal electron energy of 13 eV and a 1-s trapping time. (b) Same conditions as part a with the exception that a swept double-resonance pulse was used to eject all the ions except the proton-bound dimer. (c) Same conditions as part b except that a second double-resonance pulse was applied 40 ms prior to detection to cause the proton-bound dimer to undergo CID.

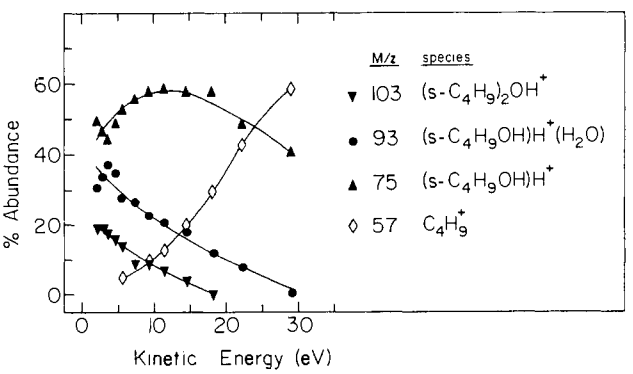

Figure 3. Product ion distribution from CID on the proton-bound dimer of *sec*-butyl alcohol: $(sec\text{-}C_4H_9OH)H^+(sec\text{-}C_4H_9OH)$.

(7) Ridge, D. P.; Beauchamp, J. L. *J. Am. Chem. Soc.* **1971**, *93*, 5925.
(8) Beauchamp, J. L.; Dunbar, R. C. *J. Am. Chem. Soc.* **1970**, *92*, 1477.
(9) Beauchamp, J. L.; Caserio, M. C. *J. Am. Chem. Soc.* **1972**, *94*, 2638.
(10) (a) Beauchamp, J. L. *J. Am. Chem. Soc.* **1969**, *91*, 5925. (b) Beauchamp, J. L.; Caserio, M. C.; McMahon, T. B. *J. Am. Chem. Soc.* **1974**, *96*, 6243.

Scheme I

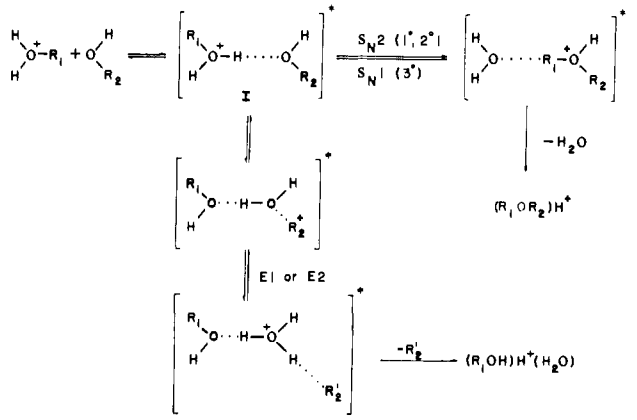

rearrangements become more important at low collision energies. High RF levels generate almost exclusively simple cleavage products.

Results and Discussion

(A) Ion–Molecule Chemistry of Aliphatic Alcohols and Formation of Proton-Bound Dimers. The ion–molecule chemistry of aliphatic alcohols has been studied previously in great detail.[7-12] It suffices to say that proton transfer from fragment ions, generated by electron impact, to the alcohol results in formation of ROH_2^+, where R includes methyl, ethyl, *n*-propyl, isopropyl, *n*-butyl, *sec*-butyl, *tert*-butyl, and *tert*-pentyl. Protonated alcohols react with their parent neutral by nucleophilic displacement of H_2O and by elimination of an olefin, reactions 2 and 3. The latter process is analogous to the acid-catalyzed dehydration of alcohols occurring in solution. Intermediate I in reactions 2 and 3 represents a loosely bound ion–molecule complex held together by electrostatic attraction of the ion with the permanent and ion-induced dipole of the neutral alcohol as well as by hydrogen bonding. As written, this intermediate can be visualized as being common to both reactions; however, any reorganization thereafter may yield specific intermediates for each reaction. Recent EB flow reactor[11] and FT/MS[12] studies on *sec*-butyl alcohol and methanol, respectively, provide strong evidence that primary and secondary alcohols react by a backside displacement mechanism as depicted in Scheme I. Tertiary alcohols are believed to react by either a frontside displacement or S_N1 mechanism. The competing acid-catalyzed dehydration involves a 1,*n* (n = 2, 3) elimination.

$$ROH_2^+ + ROH \rightarrow \underset{\text{I}}{[(ROH)_2H^+]^\dagger} \rightarrow R_2OH^+ + H_2O \quad (2)$$

$$ROH_2^+ + ROH \rightarrow \underset{\text{I}}{[(ROH)_2H^+]^\dagger} \rightarrow (ROH)H^+(H_2O) + \text{olefin} \quad (3)$$

The product of reaction 3 represents a proton-bound dimer of the alcohol and water. A simple displacement of H_2O by the more strongly basic alcohol, reaction 4, results in the formation of a proton-bound alcohol dimer. Other routes to stable proton-bound alcohol dimer formation are also available.[2-7]

$$(ROH)H^+(H_2O) + ROH \rightarrow \underset{\text{II}}{(ROH)H^+(ROH)} + H_2O \quad (4)$$

(B) Comparison of CID to Ion–Molecule Reactions. Consider the proton-bound dimer intermediate, I, activated with internal vibrational energy, $E^\dagger$. The unimolecular decomposition pathways available to this species are also available to the stable proton-bound dimer, structure II in reaction 4, after it has been vibrationally and rotationally excited to the same energy by colliding it with a neutral, nonreactive target molecule. Identical product distributions should result for both activated species if their internal energies, denoted by $E^\dagger$, are the same. Otherwise, the excited complexes may have different structures or energetically isolated isomeric forms.[13]

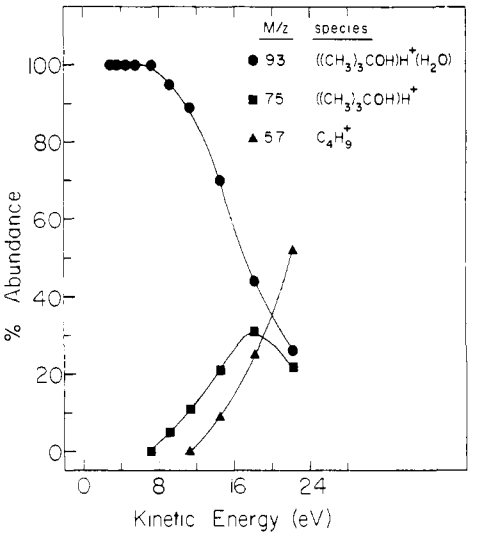

Figure 4. Product ion distribution from CID on the proton-bound dimer of *tert*-butyl alcohol: $(t\text{-}C_4H_9OH)H^+(t\text{-}C_4H_9OH)$.

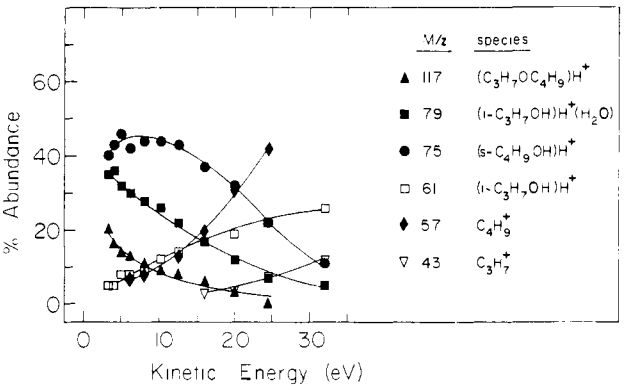

Figure 5. Product ion distribution from CID on the proton-bound dimer of isopropyl and *sec*-butyl alcohol: $(i\text{-}C_3H_7OH)H^+(sec\text{-}C_4H_9OH)$.

On the basis of a proton-bridged intermediate structure, we fully expected to observe CID reactions 5–8 for all proton-bound alcohol dimers investigated (excepting neopentyl alcohol in reaction 8[14]).

$$[(ROH)H^+(ROH)] \xrightarrow{\text{CID}} R^+ + ROH + H_2O \quad (5)$$

$$[(ROH)H^+(ROH)] \xrightarrow{\text{CID}} (ROH)H^+ + ROH \quad (6)$$

$$[(ROH)H^+(ROH)] \xrightarrow{\text{CID}} R_2OH^+ + H_2O \quad (7)$$

$$[(ROH)H^+(ROH)] \xrightarrow{\text{CID}} (ROH)H^+(H_2O) + \text{olefin} \quad (8)$$

The collision-induced decompositions of $(ROH)H^+(ROH)$ where R = *n*-propyl, *n*-butyl, *tert*-butyl, and *tert*-pentyl, however, do not yield all the products observed from bimolecular reactions of the corresponding protonated alcohol. Ions corresponding to loss of

(11) Hall, D. G.; Gupta, G.; Morton, T. H. *J. Am. Chem. Soc.* **1981**, *103*, 2416.

(12) Kleingold, J. C.; Nibbering, N. M. M. *Org. Mass Spectrom.* **1982**, *17*, 136.

(13) Alternatively, the chemically activated intermediate may exhibit apparent nonstatistical behavior in contrast to the collisionally excited species, whose internal energy would be randomly deposited. For more detail see: Chesnavich, N. J.; Bowers, M. T. In "Gas Phase Ion Chemistry"; Bowers, M. T., Ed.; Academic Press: New York, 1979. Bunker, D. L.; Hase, W. L. *J. Chem. Phys.* **1973**, *59*, 4621.

(14) A β elimination is not available unless isomerization occurs. The symmetric proton-bound dimer, $(neo\text{-}C_5H_{11}OH)_2H^+$, could not be generated in adequate yield because of small abundances of appropriate precursor ions, especially $(neo\text{-}C_5H_{11}OH)H^+$. Mixed dimers of neopentyl and *n*-propyl or *sec*-butyl alcohol, however, are readily produced from a mixture of both alcohols.

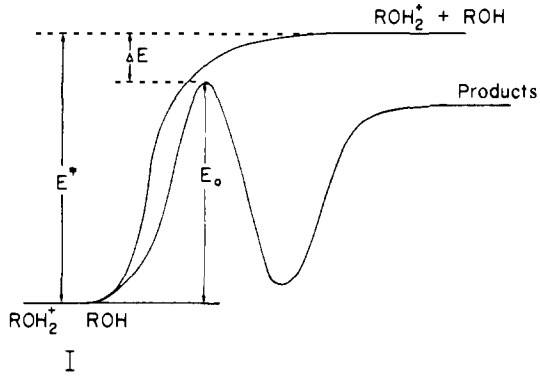

Figure 6. Hypothetical potential surface for unimolecular decomposition of proton-bridged intermediate I with internal energy E.

H_2O and propene or H_2O and butene were not observed when $(n\text{-}C_3H_7OH)H^+(n\text{-}C_3H_7OH)$ or $(n\text{-}C_4H_9OH)H^+(n\text{-}C_4H_9OH)$ were accelerated to kinetic energies in the range between 0 and 30 eV, respectively. As a further example, a plot of ion abundance vs. kinetic energy for $(t\text{-}C_4H_9OH)H^+(t\text{-}C_4H_9OH)$ shown in Figure 4 reveals that reaction 7 is not observed. These unexpected results for primary and tertiary alcohols contrast those for secondary alcohols shown in Figures 3 and 5. Proton-bound dimers of isopropyl alcohol and *sec*-butyl alcohol, when collisionally activated, dissociate via all four pathways generalized by reactions 5–8.

One could rationalize these results as evidence for different isomeric structures for the vibrationally activated intermediate I and the collisionally activated dimer II. Referring to the potential energy surface diagram in Figure 6, however, we can offer a more reasonable explanation by noting the amount of energy required to surmount a central activation barrier relative to the energy necessary to simply cleave the O–H bond bridging both alcohols. If this energy difference, ΔE, is small, indicating a high activation barrier for rearrangement, and if the internal energy of the dimer is greater than or equal to $E^\dagger$, dissociation by simple cleavage of the bridging O–H bond would be expected to be must faster than by rearrangement with loss of H_2O or the olefin. The smaller the energy gap, ΔE, the more difficult it is to selectively deposit energy into the ion below $E^\dagger$ and yet above the central energy barrier so that a specific reaction pathway is induced. In the case of *n*-propyl and *n*-butyl alcohol, for example, only simple cleavage to form the protonated alcohols is observed at low energy. From this we infer that the central barriers leading to loss of H_2O and the olefin are high, giving rise to an energy gap, ΔE, of only a couple of kilocalories. In the reaction $(n\text{-}C_3H_7OH)H^+ + n\text{-}C_3H_7OH$ only approximately 2 in every 100 collisions lead to products other than proton transfer or simply reverting to reactants.[15] This low efficiency offers direct evidence in support of the above conclusion. The tertiary alcohols, on the other hand, appear to have sufficiently low barriers to olefin elimination since the cross section for CID is substantial even at collision energies below $E^\dagger$. Loss of H_2O, however, is not as favorable a reaction. The slow rate at which the protonated di-*tert*-butyl ether is generated by ion–molecule reaction also conforms to the existence of a high central barrier along the reaction coordinate.[16]

It would appear that the nucleophilic substitution product in Scheme I can be obtained via intermediate I formed by either ion–molecule reaction or excitation of a stable proton-bound dimer. It is not absolutely necessary that the gas-phase reactants orient themselves such that they immediately resemble the transition-state geometry, although this may occur. The initially formed complex appears to be long-lived such that internal vibrations and rotations can accommodate the proper alignment of the reactant molecules. We cannot be sure, however, that in the case of *sec*-butyl alcohol loss of H_2O by CID results in retention of configuration.

(C) Comparison of CID to Multiphoton Dissociation. These above conclusions can be assessed in greater detail by noting the comparisons between multiphoton and collision-induced dissociation pathways listed in Table I. The CID results refer to observed low-energy-threshold product distributions and are established at a signal-to-noise level of ~2:1. The multiphoton dissociation (MPD) data were obtained by monitoring the products arising from sequential absorption of infrared light by proton-bound dimers. This method incorporates energy into the ion in small increments (~0.1 eV). Both experiments can be considered a series of activation and deactivation steps that ultimately lead to fragmentation.[17] Sizable deuterium isotope effects are seen with MPD, which makes it a sensitive probe of the lowest-energy decomposition pathway.[18] Multiple sets of products arising from low-power infrared activation are therefore atypical yet, suprisingly, they are observed for a few proton-bound alcohol dimers. Beauchamp et al.[4] suggest that the multiple products result from an isomerization in the transition state to yield a more stable proton-bound dimer (reaction 9) as opposed to the unlikely sit-

$$(ROH)H^+(ROH) \xrightarrow[k_1]{nh\nu} [H_2O{\cdot\cdot}R^+{\cdot\cdot}ROH]^\dagger \xrightarrow[k_2]{}$$
$$[H_2O{\cdot\cdot}R'^+{\cdot\cdot}ROH]^\dagger \rightarrow [(R'OH)H^+(ROH)]^\dagger \rightarrow \text{products} \quad (9)$$

uation that each of the products has the identical activation energy. This isomerization is implicated, for example, for $(n\text{-}C_3H_7OH)_2H^+$, dimer **3** in Table I, by the production of three products.

We observe several products including protonated diisopropyl ether when R = $i\text{-}C_3H_7$ (dimer **4**). We do not detect, however, any rearrangement (or isomerization) with the proton-bound dimers of *n*-propyl alcohol and *n*-butyl alcohol. This indicates that CID is presently not as sensitive a technique as MPD in probing the lowest-energy reaction pathways with high activation barriers. More than one product is also observed by MPD for proton-bound *sec*-butyl alcohol dimers. The correspondence between MPD and CID for dimers **6** and **7** is quite good with both techniques yielding a product ratio of ~2:1 in favor of elimination over substitution. Again, reaction 9 can be invoked to explain the MPD results.

Proton-bound dimers of tertiary alcohols **8**, **9**, and **10** in Table I dissociate by CID at low internal energies exclusively by ionic dehydration (reaction 8). The lack of correspondence between MPD and CID for dimers **8** and **10**, but not **9**, is peculiar. We can only speculate here that the MPD approach induces an isomerization (perhaps state selective) not accessible by collisional activation. Even so, the MPD results for *sec*-butyl alcohol dimers **6** and **7** suggest that isomerization of *sec*-butyl alcohol to *tert*-butyl alcohol via reaction 9 actually enhances the rate of elimination. This is not consistent with the MPD data obtained for proton-bound *tert*-butyl alcohol dimers (cf. dimers **8** and **10**). In addition, EB flow reactor studies by Morton et al. do not support an isomerization of *sec*-butyl to *tert*-butyl since no *tert*-butoxybutane was detected after neutralization of the protonated ether.[11]

The mixed proton-bound dimer of neopentyl and *n*-propyl alcohols (dimer **12**) offers some evidence, albeit inconclusive, of a collision-induced isomerization. Loss of C_5H_{10} by the collision-induced dehydration of $(n\text{-}C_3H_7OH)H^+(neo\text{-}C_5H_{11}OH)$ can occur by isomerization of neopentyl to *tert*-pentyl followed by a 1,2

(15) The ion–molecule collision frequency is calculated with the average-dipole orientation theory: Su, T.; Bowers, M. T. *Int. J. Mass Spectrom. Ion Phys.* **1973**, *12*, 347. The locking parameter was determined from a plot found in Su and Bowers: Su, T.; Bowers, M. T. In "Gas Phase Ion Chemistry"; Bowers, M. T., Ed.; Academic Press: New York, 1979; p 94. $k_{ado} = 1.7 \times 10^{-9}$ cm^3 molecule^{-1} s^{-1} for $(n\text{-}C_3H_7OH)H^+$. The experimental rate constant $k_{exptl} = (3.2 \pm 1) \times 10^{-11}$ cm^3 molecule^{-1} s^{-1}.

(16) The suppression of S_N2 reaction rates by steric hindrance due to alkyl groups on the substrate has been well-documented for both gas-phase and condensed-phase systems. Olmstead, W. N.; Brauman, J. I. *J. Am. Chem. Soc.* **1977**, *99*, 4219. Pellerite, M. J.; Brauman, J. I. *Ibid.* **1980**, *102*, 5993. Ingold, C. K. "Structure and Mechanisms in Organic Chemistry"; Cornell University Press: Ithaca, N.Y., 1969.

(17) Vibrational transition probabilities become important under low-energy collisions. See: Cosby, P. C.; Moran, T. F. *J. Chem. Phys.* **1970**, *52*, 6157. Cheng, M. H.; Chiang, M. H.; Gislason, E. A.; Mahan, B. H.; Tsao, C. W.; Werner, A. S. *Ibid.* **1970**, *52*, 6150. Collisions also enhance multiphoton dissociation. Woodin, R. L.; Bomse, D. S.; Beauchamp, J. L. *Chem. Phys. Lett.* **1979**, *63*, 630.

(18) Bomse, D. S.; Beauchamp, J. L. *J. Phys. Chem.* **1981**, *85*, 488.

Table I. Comparison of Unimolecular Decomposition Reactions of Proton-Bound Alcohol Dimers Obtained by FTMS CID and Multiphoton Dissociation

dimer	MPD[a]	CID
$(CH_3OH)H^+(CH_3OH)$ (1)	H_2O[b]	[c]
$(C_2H_5OH)H^+(C_2H_5OH)$ (2)	H_2O	[c]
$(n\text{-}C_3H_7OH)H^+(n\text{-}C_3H_7OH)$ (3)	$n\text{-}C_3H_7OH$ (0.71) H_2O (0.17) C_3H_6 (0.12)	$n\text{-}C_3H_7OH$
$(i\text{-}C_3H_7OH)H^+(i\text{-}C_3H_7OH)$ (4)	H_2O	$i\text{-}C_3H_7OH + H_2O$ (0.04) $i\text{-}C_3H_7OH$ (0.50) H_2O (0.32) C_3H_6 (0.14)
$(n\text{-}C_4H_9OH)H^+(n\text{-}C_4H_9OH)$ (5)	[c]	$n\text{-}C_4H_9OH$
$(sec\text{-}C_4H_9OH)H^+(sec\text{-}C_4H_9OH)$ (6)	H_2O (0.37) C_4H_8 (0.63)	$sec\text{-}C_4H_9OH$ (0.45) H_2O (0.18) C_4H_8 (0.37)
$(i\text{-}C_3H_7OH)H^+(sec\text{-}C_4H_9OH)$ (7)	H_2O (0.37) C_4H_8 (0.63)	$i\text{-}C_3H_7OH$ (0.40) $i\text{-}C_4H_9OH$ (0.05) H_2O (0.20) C_4H_8 (0.35)
$(t\text{-}C_4H_9OH)H^+(t\text{-}C_4H_9OH)$ (8)	H_2O	C_4H_8
$(t\text{-}C_5H_{11}OH)H^+(t\text{-}C_5H_{11}OH)$ (9)	C_5H_{10}	C_5H_{10}
$(i\text{-}C_3H_7OH)H^+(t\text{-}C_4H_9OH)$ (10)	H_2O	C_4H_8
$(sec\text{-}C_4H_9OH)H^+(neo\text{-}C_5H_{11}OH)$ (11)	[c]	$neo\text{-}C_5H_{11}OH + H_2O$ (0.09) $sec\text{-}C_4H_9OH + H_2O$ (0.08) $neo\text{-}C_5H_{11}OH$ (0.42) $sec\text{-}C_4H_9OH$ (0.10) H_2O (0.11) C_4H_8 (0.20)
$(n\text{-}C_3H_7OH)H^+(neo\text{-}C_5H_{11}OH)$ (12)	[c]	$n\text{-}C_3H_7OH + H_2O$ (0.54) $n\text{-}C_3H_7OH$ (0.29) C_5H_{10} (0.17)

[a] Multiphoton dissociation data taken from ref 4. Numbers in parentheses denote product distributions where more than one product is observed. [b] Reactions are designated by the loss of the neutral fragment in the reaction. Refer to reactions 5–8 in the text. [c] Experiment not performed.

elimination of 2-methyl-2-butene. One cannot rule out the possibility, however, of direct 1,3 elimination of 1,1-dimethylcyclopropane. Dimer **11** did not undergo this fragmentation. We postulate that relative carbonium ion stabilities reflect the rate at which isomerization occurs. Therefore, we expect that $k_1(R^+ = sec\text{-butyl}) > k_1(R^+ = \text{neopentyl})$ in reaction 9.[19] The relative difference in k_1's for two primary alcohols should be considerably less as reflected by the neutral loss of C_5H_{10} from dimer **12**.

A further consideration of the data in Table I is the relative amounts of simple cleavage products observed. Systems containing primary alcohols exhibit the highest abundance of simple-cleavage products at low threshold energies. Tertiary alcohols produce only rearrangement peaks at threshold, whereas secondary alcohols fall somewhere between primary and tertiary. This trend is consistent with our view of a decrease in the energy of activation, for dehydration of alcohol dimers, with an increase of branching at the α carbon (reaction 8).

(D) Effects of Multicollisions. Incomplete conversion of the proton-bound dimer to products is evidence for nonactivating collisions and dimers failing to undergo collision during the CID interaction period. Increasing the CID interaction time enhances the daughter ion abundances but may also alter their distribution because sufficient time has elapsed for them to react with the neutral alcohol. Reducing the interaction time decreases the CID efficiency and appears to lower the amount of internal energy acquired by the ions. For example, the distribution of products obtained by CID for the proton-bound dimer of *n*-propyl alcohol as a function of translational energy is shown in Figure 7. Only two products are observed and correspond to the simple cleavage reactions 5 and 6. Two sets of curves are presented in Figure 7. The first set pertains to a CID interaction time of 40 ms (solid curve). Here reaction 6 occurs exclusively at ion kinetic energies below about 7 eV. Its threshold is at 0.6 eV in the center of mass

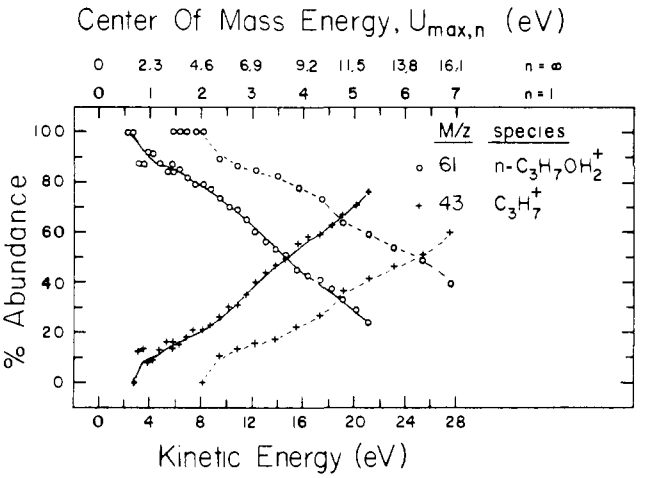

Figure 7. Product ion distribution from the proton-bound dimer of *n*-propyl alcohol, $(n\text{-}C_3H_7OH)_2H^+$, as a function of the reactant ion kinetic energy. Solid curve obtained with a 40-ms CID interaction time. Dashed curve obtained with a 4-ms interaction time.

(CM) frame, yet reaction 6 is endothermic by 1.3 eV.[20] The second set of curves is obtained with a 4-ms interaction time (dashed line) and shows a dramatic shift of the low-energy thresholds and curve crossover point to higher lab energies. This strongly suggests that multiple collisions are occurring during the 40-ms interaction period.

The onset for reaction 6 with a 4-ms interaction time is 1.4 ± 0.2 eV (CM) and this agrees well with the reported[4] bond energy $D(n\text{-}C_3H_7OH^+{}_2 - n\text{-}C_3H_7OH) = 1.3$ eV. An expression (eq 10)

$$U_{max} = K_0\left(\frac{m_1 + m_2}{2m_1 + m_2}\right) \quad (10)$$

(19) In contrast, isomerization rates (k_2) should give opposite results. Conversion of $sec\text{-}C_4H_9^+$ to $t\text{-}C_4H_9^+$ requires an endothermic 1,3-methyl shift plus a 1,2-hydride shift; however, the process $neo\text{-}C_5H_{11}^+$ to $t\text{-}C_5H_{11}^+$ is accomplished in one exothermic step.

(20) Thermochemical results indicate that the dimer dissociation energies $D(ROH_2^+ - R'OH)$ all lie between 30 and 33 kcal/mol.[9]

can readily be derived for the maximum amount of internal energy that can be obtained by an ion after being accelerated to a kinetic energy K_0 and being allowed to undergo, in the limit, an infinite number of collisions.[21] The masses of the ion and target are given by m_1 and m_2, respectively. Since most of the energy is acquired by the ion in the first few collisions, eq 10 should be satisfied (only at threshold) under experimental conditions where several collisions are occurring. The threshold for reaction 6 with a 40-ms interaction time and argon as the target gas is calculated at 1.3 ± 0.2 eV where K_0 = 2.3 eV. A threshold of 0.6 eV would incorrectly be determined if a single collision were assumed. The agreement is excellent but the determination of the threshold is subject to considerable error. Further modeling will allow us to establish the functional dependence of ion abundance on kinetic energy so that dissociation limits of greater accuracy can be obtained.

When the collision gas is turned off to the cell only very weak, sporadic CID signals (above 16 eV lab energy) are observed. This implies that collisions with the neutral alcohol do not contribute significantly to the CID spectrum.

The overall effects from using long interaction times are the enhancement of signal to noise and the ability to place more energy into the ion with use of lower kinetic energies. We do not expect, therefore, a radical alteration of the shapes of the product distribution curves but rather merely a simple shift along the energy axis. So far we have observed no indication to the contrary.

Implications for Further Study

The present study raises some important questions as to whether low-energy collision-induced dissociation performed in a Fourier-transform mass spectrometer can be used for accurate structural information. Although the salient differences between results obtained by MPD and CID can for the most part be explained by the greater energy imparted by CID even at the threshold of our signal to noise, they cannot be unequivocably explained for even such a well-characterized system as the gas-phase positive ion chemistry of aliphatic alcohols. Presently, therefore, we are developing a theory for the collision process and making comparisons with other related techniques.[21,22] These initial studies are necessary before the technique is applied to other systems. For example, the gas-phase ion chemistry of metal ions with organic molecules is of considerable interest to us.[24] A knowledge of the structures of organometallics generated in situ is important for elucidating many of the complex reaction mechanisms. Comparisons of CID fragmentations with ion–molecule chemistry, exemplified in this study of proton-bound dimers, will help us deduce their structures.

Preliminary results on the copper-ion-bound dimer of *tert*-butyl alcohol, for example, Figure 8, correlate well with those obtained here for the proton-bound dimer. Low-energy CID of (t-C_4H_9OH)Cu^+(t-C_4H_9OH) yields product ions corresponding to loss of H_2O (M/z 193), C_4H_8 (M/z 155), and t-C_4H_9OH (M/z 137), which conforms to the chemistry observed by the monomer, given by reactions 11 and 12. However, other organometallic

$$Cu(t\text{-}C_4H_9OH)^+ + t\text{-}C_4H_9OH \rightarrow \underset{M/z\ 193}{(C_4H_8)Cu^+(t\text{-}C_4H_9OH)} + H_2O \quad (11)$$

$$Cu(t\text{-}C_4H_9OH)^+ + t\text{-}C_4H_9OH \rightarrow \underset{M/z\ 155}{(H_2O)Cu^+(t\text{-}C_4H_9OH)} + C_4H_8 \quad (12)$$

systems give only simple bond-cleavage products where rearrangements are expected. For example, $Cu(CH_3COC_2H_5)^+$ and $Al(C_2H_5OH)^+$ are observed[23] to undergo unimolecular fragmentation of the metal–ligand bond yielding Cu^+ and Al^+, respectively. The observation of reactions 13[24] and 14[25] suggests,

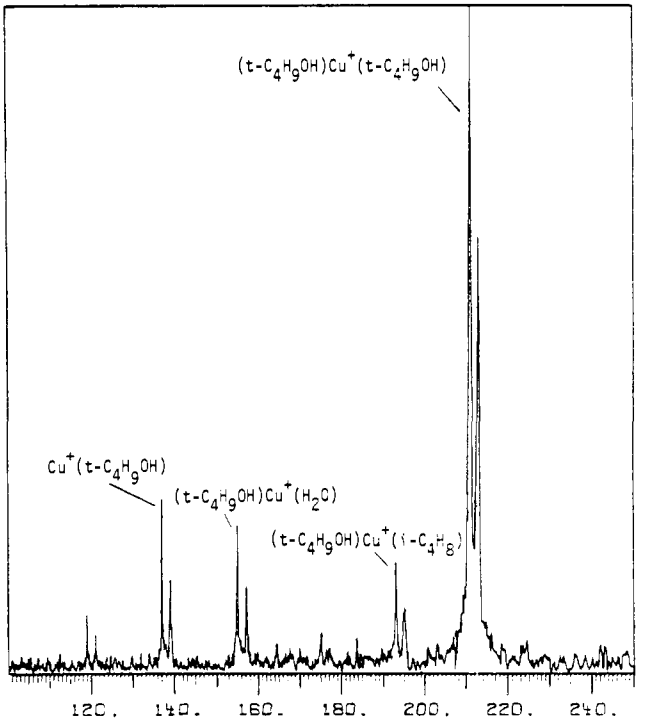

Figure 8. Mass spectrum arising from the collision-induced dissociation of (t-C_4H_9OH)Cu^+(t-C_4H_9OH).

however, that loss of H_2O and C_2H_4 should be observed by low-energy CID.

$$Cu^+ + CH_3COC_2H_5 \rightarrow Cu(C_4H_6)^+ + H_2O \quad (13)$$

$$Al^+ + C_2H_5OH \rightarrow Al(H_2O)^+ + C_2H_4 \quad (14)$$

In summary, low-energy collision spectroscopy provides a method for monitoring the unimolecular decomposition of polyatomic ions as a function of ion internal energy. Low-energy product distribution profiles can be used to examine relative heights of activation barriers in the unimolecular decomposition exit channel. In essence, these curves facilitate the examination of ions in terms of their structure and energetics. Structural isomers (for example **3** and **4**; **5**, **6**, and **8**; **7** and **10**) are easily distinguished on the basis of their product distribution curves. In addition, we have found that products of FT/MS collision-induced dissociation of several proton-bound dimers are identical with those obtained by exothermic bimolecular reactions of the dimer constituents, but sometimes not every ion is observed. These results represent situations where activation barriers are too close to the potential energy of the reactants.

Finally, the ease of dehydration of alcohols in the gas phase appears to follow the same order observed for their acid-catalyzed dehydration in solution: tertiary > secondary > primary. On the whole, the comparison between the MPD and CID results is good, but it illustrates that CID samples higher internal energies than MPD. Further comparisons of this type will be crucial in evaluating each method, but it is certain that photodissociation[25] and collision-induced dissociation techniques will afford complementary information regarding ion structures and energetics.

Acknowledgement is made to the donors of the Petroleum Research Fund, administered by the American Chemical Society. The authors also wish to thank the National Science Foundation for providing funds to purchase the FT/MS instrument. Finally, we thank the Nicolet Corp. for their technical assistance.

Registry No. n-C_3H_7OH, 71-23-8; i-C_3H_7OH, 67-63-0; n-C_4H_9OH, 71-36-3; *sec*-C_4H_9OH, 78-92-2; t-C_4H_9OH, 75-65-0; t-$C_5H_{11}OH$, 75-85-4; *neo*-$C_5H_{11}OH$, 75-84-3.

(21) Cody, R. B. Ph.D. Thesis, Purdue University, 1982.
(22) McLuckey, S. A.; Cody, R. B.; Sallans, L. A.; Burnier, R. C.; Freiser, B. S.; Cooks, R. G., to be published.
(23) Burnier, R. C.; Freiser, B. S., unpublished results.
(24) Burnier, R. C.; Byrd, G. D.; Freiser, B. S. *Anal. Chem.* **1980**, *52*, 1641.
(25) Uppal, J. S.; Staley, R. H. *J. Am. Chem. Soc.* **1982**, *104*, 1229.
(26) For a description of photodissociation techniques other than MPD, see: Dunbar, R. C. In "Gas Phase Ion Chemistry"; Bowers, M. T., Ed.; Academic Press: New York, 1979.